Chapter 4

DFT And Thermodynamics

Density-functional theory has nowadays become a standard tool for electronic structure calculations. Using this technique a detailed insight into the microscopic regime can be obtained. On the other hand one would like to understand and describe material science problems, like in this work heterogenous catalysis, which are clearly on a macroscopic time and length scale. To explain macroscopic phenomena on the basis of a microscopic understanding a huge range of time and length scales needs to be covered. To find an appropriate linking between the micro-, meso- and macroscopic regime is referred to as *multiscale modeling* approach [27, 28]. In Fig. 4.1 the time and length scales for the different regimes are schematically shown. Also the different

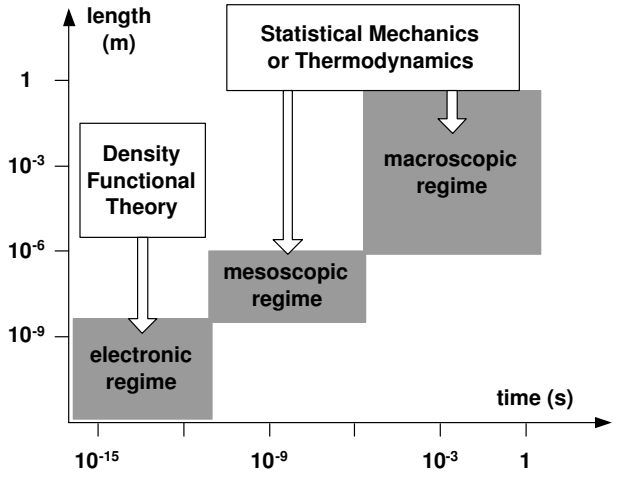

Figure 4.1: Schematic representation of the time and length scales for the micro-, meso- and macroscopic regime. Several methods have been developed to tackle problems within a certain regime. In the multiscale modeling approach an appropriate linking between the different regimes is developed, so that information obtained in the microscopic regime can, e.g., be transferred into the meso- and macroscopic regime (from Ref. [27]). The present study concentrates on a linking between the electronic and macroscopic regimes.

methods used in this work to describe the different regimes are indicated. As already mentioned DFT is used for the electronic (microscopic) regime. The results from DFT are then combined with concepts from thermodynamics and statistical mechanics to reach the meso- and macroscopic regime. Since the results obtained within DFT do not rely on semi-empirical or fitted parameters they are referred to *first principle* or *ab initio*. Using DFT or other first-principle electronic structure theory results as input to macroscopic theories is similarly classified as first-principle (*ab initio*).

This Chapter focuses on the linking between DFT and thermodynamics, whereas in Chapter 5 a combination of DFT and statistical mechanics is described.

4.1 Ab Initio Atomistic Thermodynamics

In results obtained from electronic structure calculations temperature and pressure effects are not included, i.e. all evaluated physical quantities are strictly only valid at $T = 0\,\mathrm{K}$ and $p = 0\,\mathrm{atm}$. The effect of temperature on the atomic positions can be obtained, though, by evaluating the total energy as a function of the nuclear positions, $\{\mathbf{R}_A\}$, on the Born-Oppenheimer surface (cf. Section 2.1). The resulting Born-Oppenheimer potential energy surface can then be used to extract further information as e.g. vibrational modes. To now actually describe situations of finite temperatures and pressures the results from DFT calculations can be used as an input to thermodynamic considerations [70–73]. The appropriate thermodynamic functions can then be evaluated over the whole temperature and pressure range.

The key quantity in studying a (T, p)-ensemble is the Gibbs free energy G

$$G(T,p) = E^{\mathrm{tot}} + F^{\mathrm{vib}} - TS^{\mathrm{conf}} + pV \quad . \tag{4.1}$$

The leading term is the total energy E^{tot}, which is directly obtained from the electronic structure calculations. The second term F^{vib} accounts for the vibrational contributions (with $F^{\mathrm{vib}} = E^{\mathrm{ZPE}} - TS^{\mathrm{vib}}$ being the vibrational free energy). The third term TS^{conf} includes configurational entropy and the last one is the pV-term. An evaluation of the different contributions to the Gibbs free energy will be exemplified below for the calculation of the surface free energy and the Gibbs free energy of adsorption.

The combination of DFT and thermodynamics is applicable to systems, that are in thermodynamic equilibrium. This implies another important concept. A system in thermodynamic equilibrium can be divided into smaller subsystems, which again are in thermodynamic equilibrium with each other. In the atomistic thermodynamics approach every subsystem can then be treated separately within DFT. This is especially useful, if infinite but homogeneous subsystems, such as bulk or gas phases acting e.g. as a reservoir, are involved [8, 9, 74–77].

The general concept of atomistic thermodynamics is exemplified here once for the calculation of the surface free energy and once for the Gibbs free energy of adsorption.

4.2 Surface Free Energy

In equilibrium, a one-component system can be fully described by its internal energy E, which depends on the entropy S, the volume V and the number of particles N in the system

$$E^{\text{bulk}} = TS - pV + N\mu \quad , \tag{4.2}$$

with μ being the chemical potential. If a homogeneous solid is cleaved, two surfaces of size A are being created. Since this process does not occur spontaneously the internal energy of the system has to increase by an amount proportional to A. The constant of proportionality is defined as the surface energy γ [78], so that the internal energy of a cleaved crystal can be written as

$$E^{\text{surf}} = TS - pV + N\mu + \gamma A \quad . \tag{4.3}$$

Introducing again the Gibbs free energy $G = E - TS + pV$ and rearranging Eq. (4.3) the surface free energy for a one-component system is defined as

$$\gamma = \frac{1}{A}[G^{\text{surf}} - N\mu] \quad , \tag{4.4}$$

where G^{surf} is the Gibbs free energy of the cleaved crystal. For a multi-component system being in equilibrium with atomic reservoirs (e.g. a surrounding gas or liquid phase environment, or a macroscopic bulk phase) the expression for the surface free energy can be written more general as

$$\gamma(T, p_i) = \frac{1}{A}\left[G^{\text{surf}} - \sum_i N_i \mu_i(T, p_i)\right] \quad . \tag{4.5}$$

G^{surf} is again the Gibbs free energy of the solid including the surface and $\mu_i(T, p_i)$ is the chemical potential of the various species i present in the system. In the following the application of Eq. (4.5) to *metal oxides* in equilibrium with a surrounding *oxygen gas phase* is discussed (cf. Fig. 4.2). All presented equations can be applied similarly to any other two-component system or easily be extended to multi-component systems. In the case of a metal oxide the surface free energy is a function of the chemical potential of the metal μ_{M} and the oxygen μ_{O}

$$\gamma(T, p) = \frac{1}{A}\left[G^{\text{surf}}(T, p, N_{\text{M}}, N_{\text{O}}) - N_{\text{M}}\mu_{\text{M}}(T, p) - N_{\text{O}}\mu_{\text{O}}(T, p)\right] \tag{4.6}$$

Here, N_{M} and N_{O} are the number of metal and oxygen atoms within the finite part of the total (infinite) system, G^{surf}, that is influenced by the created surface. With increasing distance from the surface the solid as well as the gas phase part of the total system will become equivalent to the homogeneous solid and gas phase systems represented by μ_{M} and μ_{O}. By subtracting the respective amount of the homogeneous

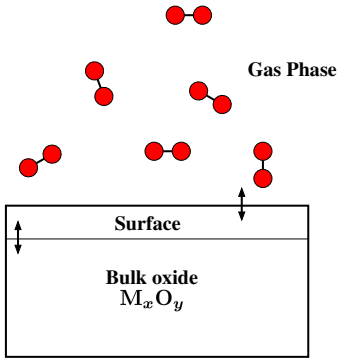

Figure 4.2: Surface in thermodynamic equilibrium with a surrounding gas phase and the underlying bulk phase. If the different phases are in thermodynamic equilibrium, their chemical potentials have to be equal. Thus the system can be divided into three subsystem, bulk oxide, surface and gas phase, the energetics of which can be treated separately within DFT.

systems from the total system these parts are effectively canceled out, so that the surface free energy can sufficiently be determined by the finite part containing N_M metal and N_O oxygen atoms. Because the surface is in equilibrium with the underlying bulk oxide, the two chemical potentials μ_M and μ_O can not be varied independently. They connect via the Gibbs free energy of the bulk oxide. In thermodynamic equilibrium this is determined by

$$x\mu_\mathrm{M} + y\mu_\mathrm{O} = g^{\mathrm{bulk}}_{\mathrm{M}_x\mathrm{O}_y}(T,p) \quad , \tag{4.7}$$

where the small g denotes the Gibbs free energy per formula unit. Substituting Eq. (4.7) into Eq. (4.6) one obtains the surface free energy depending only on the chemical potential of the oxygen μ_O

$$\gamma(T,p) = \frac{1}{A}\left[G^{\mathrm{surf}}(T,p,N_\mathrm{M},N_\mathrm{O}) - \frac{N_\mathrm{M}}{x}g^{\mathrm{bulk}}_{\mathrm{M}_x\mathrm{O}_y}(T,p) - (N_\mathrm{O} - \frac{y}{x}N_\mathrm{M})\mu_\mathrm{O}(T,p)\right] \quad . \tag{4.8}$$

The chemical potential is fully determined by the temperature and pressure conditions of the surrounding oxygen gas phase. Using Eq. (4.8) the surface free energy of any given metal oxide surface can be calculated and their thermodynamic stabilities can be compared with respect to the given gas phase conditions.

Range Of Allowed Chemical Potentials

Although the oxygen chemical potential μ_O can theoretically be varied from minus to plus infinity, it only makes sense within certain boundaries. For a metal oxide a suitable lower boundary of μ_O, which will be called the *O-poor limit*, is defined by the decomposition of the oxide into the pure metal and gas phase oxygen. In terms of thermodynamic quantities this point is reached, if the chemical potential of the metal in the considered oxide system, μ_M, becomes larger than its Gibbs free energy in the

metal bulk, $g_{\mathrm{M}}^{\mathrm{bulk}}$. This upper bound of μ_{M},

$$\mu_{\mathrm{M}} \leq g_{\mathrm{M}}^{\mathrm{bulk}} \tag{4.9}$$

can be transformed into a lower bound of μ_{O} by utilizing Eq. (4.7)

$$\mu_{\mathrm{O}}(T,p) \geq \frac{1}{y}\left(g_{\mathrm{M}_x\mathrm{O}_y}^{\mathrm{bulk}}(T,p) - x g_{\mathrm{M}}^{\mathrm{bulk}}(T,p)\right) \quad . \tag{4.10}$$

A reasonable upper bound of the chemical potential for a system describing a surface in equilibrium with a gas phase is given by such gas phase conditions, in which the gaseous component is so highly concentrated, that condensation will start on the sample at low enough temperatures. Again, for the example of a metal oxide in equilibrium with an oxygen gas phase this *O-rich limit* will be defined here as

$$\mu_{\mathrm{O}} \leq 1/2 E_{\mathrm{O}_2}^{\mathrm{tot}} \quad , \tag{4.11}$$

with $E_{\mathrm{O}_2}^{\mathrm{tot}}$ being the total energy of the oxygen gas phase. Combining Eq. (4.10) and Eq. (4.11) the range of evaluated oxygen chemical potential is given by

$$\frac{1}{y}\underbrace{\left(g_{\mathrm{M}_x\mathrm{O}_y}^{\mathrm{bulk}}(T,p) - x g_{\mathrm{M}}^{\mathrm{bulk}}(T,p) - \frac{y}{2}E_{\mathrm{O}_2}^{\mathrm{tot}}\right)}_{\simeq \Delta G_{\mathrm{M}_x\mathrm{O}_y}^{f}(0,0)} \leq \underbrace{\mu_{\mathrm{O}}(T,p) - 1/2 E_{\mathrm{O}_2}^{\mathrm{tot}}}_{\Delta\mu_{\mathrm{O}}(T,p)} \leq 0 \quad . \tag{4.12}$$

Here, $\Delta G_{\mathrm{M}_x\mathrm{O}_y}^{f}(0,0)$ is the heat of formation of the corresponding bulk oxide at $T = 0\,\mathrm{K}$. By replacing μ_{O} with $\Delta\mu_{\mathrm{O}}$ the total energy of the oxygen gas phase, $1/2E_{\mathrm{O}_2}^{\mathrm{tot}}$, which marks the upper boundary, is set as a zero reference. This can be done, because the total energy $E_{\mathrm{O}_2}^{\mathrm{tot}}$ does not depend on temperature and pressure. All (T,p)-dependent terms are summarized in $\Delta\mu_{\mathrm{O}}$, cf. Section 4.4. The lower bound is thus approximated by the heat of formation at $T = 0\,\mathrm{K}$. The temperature and pressure dependence of the lower bound introduced by $g_{\mathrm{M}_x\mathrm{O}_y}^{\mathrm{bulk}}(T,p)$ and $g_{\mathrm{M}}^{\mathrm{bulk}}(T,p)$ leads only to small deviations in the here discussed (T,p)-range. An additional advantage of defining the lower bound by $\Delta G_{\mathrm{M}_x\mathrm{O}_y}^{f}(0,0)$ is that the heat of formation is a measurable quantity, which can then also be compared to experimental results.

Surface Free Energy In The O-poor And O-rich Limit

In Eq. (4.8) the dependence of the surface free energy on the chemical potential of the oxygen gas phase is described. To substitute μ_{O} in Eq. (4.8) with the appropriate upper and lower boundaries, Eq. (4.12) is rewritten as

$$\begin{aligned} &\frac{1}{y}\left(g_{\mathrm{M}_x\mathrm{O}_y}^{\mathrm{bulk}}(T,p) - x g_{\mathrm{M}}^{\mathrm{bulk}}(T,p)\right) \leq \mu_{\mathrm{O}}(T,p) \leq \\ &\quad \leq \frac{1}{y}\left(g_{\mathrm{M}_x\mathrm{O}_y}^{\mathrm{bulk}}(T,p) - x g_{\mathrm{M}}^{\mathrm{bulk}}(T,p)\right) - \frac{1}{y}\Delta G_{\mathrm{M}_x\mathrm{O}_y}^{f}(0,0) \quad . \end{aligned} \tag{4.13}$$

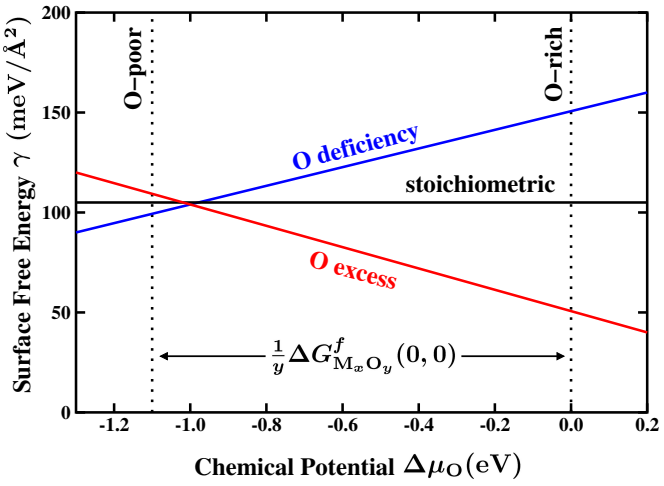

Figure 4.3: Example of plotting the surface free energy γ vs. the chemical potential of the surrounding gas phase $\Delta\mu_O$. The surface free energy of a stoichiometric surface composition will be independent of the gas phase chemical potential (black line), a surface structure with an oxygen excess (red line) will become more stable and with an oxygen deficiency (blue line) less stable with increasing gas phase chemical potential. The range of allowed oxygen chemical potential is given by the stability of the corresponding bulk oxide, $\frac{1}{y}\Delta G^f_{M_xO_y}$.

The surface free energy in the O-poor limit is then obtained by inserting the left part of the inequality (4.13) into the expression for the surface free energy (Eq. (4.8))

$$\begin{aligned}\gamma_{\mathrm{O-poor}}(T,p) =& \frac{1}{A}\Big[G^{\mathrm{surf}}(T,p,N_M,N_O) - \frac{N_M}{x}g^{\mathrm{bulk}}_{M_xO_y}(T,p) \\ &- \left(\frac{1}{y}N_O - \frac{1}{x}N_M\right)\left(g^{\mathrm{bulk}}_{M_xO_y}(T,p) - xg^{\mathrm{bulk}}_{M}(T,p)\right)\Big] \quad .\end{aligned} \tag{4.14}$$

In the oxygen-rich limit using the right part of Eq. (4.13) yields similarly

$$\gamma_{\mathrm{O-rich}}(T,p) = \gamma_{\mathrm{O-poor}}(T,p) + \frac{1}{A}\left(\frac{1}{y}N_O - \frac{1}{x}N_M\right)\Delta G^f_{M_xO_y}(0,0) \quad . \tag{4.15}$$

Eq. (4.8) shows a linear dependence of the surface free energy on the chemical potential of the oxygen gas phase. The slope of the resulting line, $-\frac{1}{A}(N_O - \frac{y}{x}N_M)$, is only determined by the ratio and density of the two components in the system, i.e. in a stoichiometric surface termination, the surface free energy will not depend on the oxygen chemical potential, whereas an oxygen excess will lead to a lowering of γ with increasing μ_O. Respectively, an oxygen deficiency will lead to an increase in the surface free energy with increasing μ_O(cf. Fig. 4.3). The width of the stability range is determined by the stability of the bulk oxide per oxygen atom, i.e. the heat of formation $\frac{1}{y}\Delta G^f_{M_xO_y}(0,0)$.

Evaluating The Gibbs Free Energy

To quantitatively calculate the surface free energy in the O-poor and O-rich limit the Gibbs free energies (as defined in Eq. (4.1)) have to be evaluated for the different components. As already mentioned above the leading term is the total energy E^{tot}, which is obtained directly from the electronic structure calculations. In a first approach, an order of magnitude estimate of the remaining terms, the pV-term, the configurational entropy and the vibrational contribution to the surface free energy, is discussed in the following.

The contribution of the last term in Eq. (4.1), the pV-term, can be approximated by a simple dimensional analysis. Since the surface energy is calculated per surface area the pV-term will be roughly $[pV/A]$ =atm $\text{Å}^3/\text{Å}^2 \sim$ p [in atm]$10^{-3}\,\mathrm{meV/Å^2}$. Even for pressures up to $p \sim 100\,\mathrm{atm}$ the pV-contribution will thus still be less than $\sim 0.1\,\mathrm{meV/Å^2}$, which in any case will be insignificant compared to the total energy term. Therefore the contribution of the pV-term to the surface free energy can be safely neglected.

The contribution arising from the configurational entropy is not as easy to estimate and strongly depends on the investigated system. For a complete sampling of the configurational space modern statistical methods, like Monte Carlo simulations, have to be applied, which will be discussed in the following Chapter.

Focusing here on the surface energy of a well-ordered, crystalline metal oxide, nevertheless some approximations can be derived. Here the configurational entropy will mainly result from some disorder, e.g. defects, at the considered surface. From statistical mechanics this configurational entropy is given by

$$S^{\mathrm{conf}} = k_{\mathrm{B}} \ln \frac{(N+n)!}{N!\,n!} \tag{4.16}$$

for a system with N surface sites an a small number of n defects or adsorbate sites, so that $n \ll N$. With A_{site} being the surface area per site, i.e. $A = NA_{\mathrm{site}}$, the energy contribution from the configurational entropy can be written as

$$\frac{TS^{\mathrm{conf}}}{NA_{\mathrm{site}}} = \frac{k_{\mathrm{B}}T}{NA_{\mathrm{site}}} \ln \frac{(N+n)!}{N!\,n!} \quad . \tag{4.17}$$

Applying the Stirling formula ($\ln N! = N \ln N - N$) to Eq. (4.17), for $n, N \gg 1$, yields

$$\frac{TS^{\mathrm{conf}}}{NA_{\mathrm{site}}} = \frac{k_{\mathrm{B}}T}{A_{\mathrm{site}}} \left[\ln\left(1 + \frac{n}{N}\right) + \frac{n}{N} \ln\left(1 + \frac{N}{n}\right) \right] \tag{4.18}$$

Assuming that in a moderately disordered surface the ratio of (n/N) stays within 10%, Eq. (4.18) gives

$$\frac{TS^{\mathrm{conf}}}{A} \leq 0.34 \frac{k_{\mathrm{B}}T}{A_{\mathrm{site}}} \quad . \tag{4.19}$$

For temperatures up to $T = 1000\,\mathrm{K}$ and surface areas per site of about $A_{\mathrm{site}} \approx 10\,\text{Å}^2$ the configurational entropy will thus not contribute more than about $3\,\mathrm{meV/Å^2}$ to the

Gibbs free energy of the surface. To a first approximation this contribution is often also neglected, since in comparing different surface free energies changes in this order of magnitude are often insignificant. It is, however, important to note, that these approximations will not hold for systems having highly disordered surface phases. The atomistic thermodynamics approach as used in this work, on the other hand, is a *direct screening method*, i.e. it can only be used to directly compare the stability of all considered, i.e. of all plausible, structures, but not to sample the configurational space of all, ordered and disordered, structures (as in Monte Carlo simulations). Thus, highly disordered surface phases are usually not considered within this approach.

The remaining vibrational contribution F^{vib} in Eq. (4.1) can in principle be calculated using DFT. In practice this is a very time consuming procedure, since the entire phonon density of states (phonon DOS) $\sigma(\omega)$ at the surface and in the bulk has to be calculated. The free energy F contains an energy E and an entropy S term, which can be calculated via the partition function Z of the system using statistical thermodynamics [79], so that

$$\begin{aligned} F^{\text{vib}}(T, V, N_{\text{M}}, N_{\text{O}}) &= E^{\text{vib}} - TS^{\text{vib}} \\ &= -\frac{\partial}{\partial\beta} \ln Z^{\text{vib}} - Tk_{\text{B}}(\ln Z^{\text{vib}} + \beta E^{\text{vib}}) \\ &= -k_{\text{B}}T \ln Z^{\text{vib}} \quad , \end{aligned} \tag{4.20}$$

with $\beta = 1/k_{\text{B}}T$. The vibrational partition function of an N-atomic, solid system is defined as [80]

$$\begin{aligned} Z^{\text{vib}} &= \sum_{i=1}^{3N} \int \frac{d\mathbf{k}}{(2\pi)^3} \sum_{n=0}^{\infty} e^{-[n+(1/2)]\beta\hbar\omega_i(\mathbf{k})} \\ &= \sum_{i=1}^{3N} \int \frac{d\mathbf{k}}{(2\pi)^3} \frac{\exp(-1/2\beta\hbar\omega_i(\mathbf{k}))}{[1 - \exp(-\beta\hbar\omega_i(\mathbf{k})]} \end{aligned} \tag{4.21}$$

where $\omega_i(\mathbf{k})$ are the $3N$ vibrational modes. Inserting Eq. (4.21) into Eq. (4.20) and using the phonon DOS $\sigma(\omega)$ the vibrational component of the free energy can then be written as

$$F^{\text{vib}}(T, V, N_{\text{M}}, N_{\text{O}}) = \int d\omega F^{\text{vib}}(T, \omega)\sigma(\omega) \quad , \tag{4.22}$$

where the frequency dependent function $F^{\text{vib}}(T, \omega)$ in Eq. (4.22) is then defined as

$$F^{\text{vib}}(T, \omega) = \frac{1}{2}\hbar\omega + k_{\text{B}}T \ln(1 - e^{-\beta\hbar\omega}) \quad . \tag{4.23}$$

Instead of calculating the full phonon DOS it might be useful to first obtain an estimate of the magnitude of the phonon contribution to the investigated physical quantity, like in this case to the surface free energy γ. Here, the vibrational contribution, γ^{vib}, only enters as the *difference* in the vibrational energy of atoms in the surface

(contributions to $G^{\mathrm{surf}}(T, p, N_{\mathrm{M}}, N_{\mathrm{O}})$) and in the bulk (contributions to $g^{\mathrm{bulk}}_{\mathrm{M}_x\mathrm{O}_y}(T, p)$ and $g^{\mathrm{bulk}}_{\mathrm{M}}(T, p)$). This yield, e.g., in the O-poor limit

$$\begin{aligned}\gamma^{\mathrm{vib}}_{\mathrm{O-poor}}(T, V) &= \\ &= \frac{1}{A}\int d\omega F^{\mathrm{vib}}(T,\omega)\Big[\sigma^{\mathrm{surf}}(\omega) - \frac{N_{\mathrm{O}}}{y}\sigma^{\mathrm{bulk}}_{\mathrm{M}_x\mathrm{O}_y}(\omega) + \Big(\frac{x}{y}N_{\mathrm{O}} - N_{\mathrm{M}}\Big)\sigma^{\mathrm{bulk}}_{\mathrm{M}}(\omega)\Big]\end{aligned} \tag{4.24}$$

As a first estimate of the value of $\gamma^{\mathrm{vib}}_{\mathrm{O-poor}}$ the phonon DOS can be approximated by the Einstein model [80]. In the Einstein model the phonon DOS is simply a delta function at one characteristic frequency $\bar{\omega}$. Here, one characteristic frequency for each atom type is chosen, i.e. for the metal and the oxygen as well as for atoms in the bulk $\bar{\omega}^{\mathrm{bulk}}$ and at the surface $\bar{\omega}^{\mathrm{surf}}$. The vibrational free energy of the surface system can then be expressed as a sum over the different atom types

$$\begin{aligned}\int d\omega F^{\mathrm{vib}}(T,\omega)\sigma^{\mathrm{surf}}(\omega) \approx 3F^{\mathrm{vib,surf}} = \\ = 3\big[&(N_{\mathrm{O}} - N^{\mathrm{surf}}_{\mathrm{O}})F^{\mathrm{vib}}(T,\bar{\omega}^{\mathrm{bulk}}_{\mathrm{O}}) + N^{\mathrm{surf}}_{\mathrm{O}}F^{\mathrm{vib}}(T,\bar{\omega}^{\mathrm{surf}}_{\mathrm{O}}) \\ &+ (N_{\mathrm{M}} - N^{\mathrm{surf}}_{\mathrm{M}})F^{\mathrm{vib}}(T,\bar{\omega}^{\mathrm{bulk}}_{\mathrm{M}}) + N^{\mathrm{surf}}_{\mathrm{M}}F^{\mathrm{vib}}(T,\bar{\omega}^{\mathrm{surf}}_{\mathrm{M}})\big] \quad ,\end{aligned} \tag{4.25}$$

where $N^{\mathrm{surf}}_{\mathrm{O}}$ and $N^{\mathrm{surf}}_{\mathrm{M}}$ are the number of oxygen, resp. metal atoms right at the surface. For the other terms the vibrational free energy is similarly

$$F^{\mathrm{vib,bulk}}_{\mathrm{M}_x\mathrm{O}_y} \approx xF^{\mathrm{vib}}(T,\bar{\omega}^{\mathrm{bulk}}_{\mathrm{M}}) + yF^{\mathrm{vib}}(T,\bar{\omega}^{\mathrm{bulk}}_{\mathrm{O}}) \tag{4.26}$$

and

$$F^{\mathrm{vib,bulk}}_{\mathrm{M}} \approx F^{\mathrm{vib}}(T,\bar{\omega}^{\mathrm{bulk}}_{\mathrm{M}}) \quad . \tag{4.27}$$

Substituting Eq. (4.25) – (4.27) into Eq. (4.24) results in the following expression for the vibrational contribution to the surface free energy of a metal oxide

$$\begin{aligned}\gamma^{\mathrm{vib}}_{\mathrm{O-poor}}(T, V) = &\frac{3}{A}\Big(N^{\mathrm{surf}}_{\mathrm{M}}\big[F^{\mathrm{vib}}(T,\bar{\omega}^{\mathrm{surf}}_{\mathrm{M}}) - F^{\mathrm{vib}}(T,\bar{\omega}^{\mathrm{bulk}}_{\mathrm{M}})\big] \\ &+ N^{\mathrm{surf}}_{\mathrm{O}}\big[F^{\mathrm{vib}}(T,\bar{\omega}^{\mathrm{surf}}_{\mathrm{O}}) - F^{\mathrm{vib}}(T,\bar{\omega}^{\mathrm{bulk}}_{\mathrm{O}})\big]\Big) \quad .\end{aligned} \tag{4.28}$$

In Fig. 4.4 $\gamma^{\mathrm{vib}}_{\mathrm{O-poor}}$ is shown for temperatures up to 1000 K, using $\bar{\omega}^{\mathrm{bulk}}_{\mathrm{M}} = 20\,\mathrm{meV}$ and $\bar{\omega}^{\mathrm{bulk}}_{\mathrm{O}} = 70\,\mathrm{meV}$ as a coarse estimate for the characteristic frequencies of the metal and oxygen bulk atoms (considering as example for the characteristic frequencies PdO [81]). Since the change of the vibrational modes at the surface might be quite significant due to the change in coordination, the characteristic frequencies at the surface are allowed to vary ±50 % from the bulk values (two black, solid lines in Fig. 4.4). The surface area A is set to $20\,\mathrm{Å}^2$ having one metal and one oxygen atom at the surface, i.e. $N^{\mathrm{surf}}_{\mathrm{M}} = N^{\mathrm{surf}}_{\mathrm{O}} = 1$. Changing the characteristic frequencies for the bulk atoms by ±50 % does not change the magnitude of the vibrational contribution

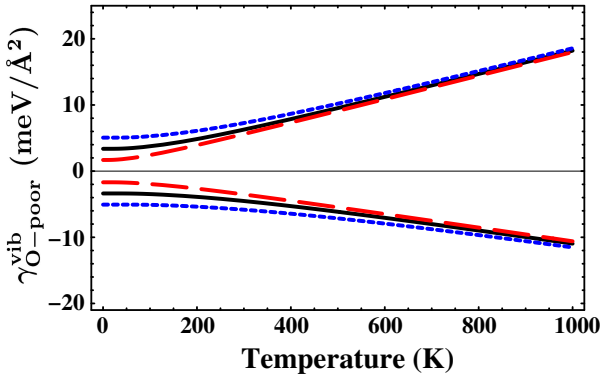

Figure 4.4: Estimate of the vibrational contribution to the surface free energy in the O-poor limit. The Einstein model has been used to approximate the phonon DOS. To account for the change of the vibrational modes of atoms at the surface compared to bulk atoms, the characteristic frequencies of the surface atoms are varied ±50 % compared to the bulk frequencies. The dashed-red and dotted-blue lines represent an additional ±50 % variation of the selected characteristic frequencies of the bulk atoms.

very much, as can be seen from the dashed-red (-50 %) and dotted-blue (+50 %) curves in Fig. 4.4. Here again the frequencies at the surface are varied by ±50 % with respect to the bulk value.

It becomes obvious, that even for temperatures up to 1000 K the vibrational contribution to the surface free energy is rather moderate. Nevertheless it has to be stressed, that this might not in general apply to other surfaces. But the scheme for obtaining a first coarse estimate of the order of magnitude of the vibrational contribution can just as well be adapted to other systems. Also the accuracy needed in the surface free energy is an important factor. If in any case the vibrational contribution turns out not to be negligible, the calculation of the phonon DOS would become necessary to include this contribution correctly.

The discussion shows that for the surface free energy of a metal oxide surface the total energy E^{tot} is indeed the leading term, whereas for the other contributions, F^{vib}, TS^{conf} and pV, a rough estimate showed, that they are only of minor importance for the present applications. Again it should be stressed, that this not necessarily valid in general, but has to carefully tested for every new system.

4.3 The Gibbs Free Energy Of Adsorption

4.3.1 One-Component Gas Phase

As a second example for combining DFT and thermodynamics the Gibbs free energy of adsorption ΔG^{ads} for a metal surface in equilibrium with a surrounding gas phase is evaluated in this Section. The Gibbs free energy of adsorption can be used to compare

the stability of different adsorbate phases depending on the gas phase conditions. The stability of the different adsorbate phases is compared with respect to the clean metal surface. For an adsorbate phase in equilibrium with an oxygen gas phase, ΔG^{ads} is given by

$$\begin{aligned}\Delta G^{\text{ads}}(T,p) &= \gamma_{\text{M}}(T,p,N'_{\text{M}}) - \gamma_{\text{O@M}}(T,p,N_{\text{M}},N_{\text{O}}) \\ &= -\frac{1}{A}\left(G^{\text{surf}}_{\text{O@M}}(T,p) - G^{\text{surf}}_{\text{M}}(T,p) - \Delta N_{\text{M}}\mu_{\text{M}}(T,p) - N_{\text{O}}\mu_{\text{O}}(T,p)\right) \quad ,\end{aligned} \tag{4.29}$$

where $G^{\text{surf}}_{\text{O@M}}$ is the Gibbs free energy of the metal surface with N_{O} adsorbed oxygen atoms, $G^{\text{surf}}_{\text{M}}$ is the Gibbs free energy of the clean metal surface and μ_{O} is the chemical potential of the oxygen atoms. If the number of metal atoms in the adsorbate phase and the clean surface are not equal, i.e. $\Delta N_{\text{M}} = N_{\text{M}} - N'_{\text{M}} \neq 0$, the excess/deficiency atoms are taken from/put into a bulk reservoir, represented by the gibbs free energy of the bulk phase, $g^{\text{bulk}}_{\text{M}}$. A is again the surface area. Substituting μ_{O} by $\Delta\mu_{\text{O}}$, cf. Eq. (4.38), yields

$$\begin{aligned}\Delta G^{\text{ads}}(\Delta\mu_{\text{O}}) &= -\frac{1}{A}\left(G^{\text{surf}}_{\text{O@M}} - G^{\text{surf}}_{\text{M}} - \Delta N_{\text{M}} g^{\text{bulk}}_{\text{M}} - N_{\text{O}}(1/2E^{\text{tot}}_{\text{O}_2} + \Delta\mu_{\text{O}})\right) \\ &= -\frac{N_{\text{O}}}{A}\Delta G^{\text{bind}}_{\text{O@M}} + \frac{N_{\text{O}}}{A}\Delta\mu_{\text{O}} \quad ,\end{aligned} \tag{4.30}$$

with $\Delta G^{\text{bind}}_{\text{O@M}}$ being the binding energy per adsorbed oxygen atom. The Gibbs free energy of adsorption shows a linear dependence on the chemical potential of the gas phase. The slope depends only on the coverage, i.e. the number of oxygen atoms N_{O} per surface area A. A structure with a higher coverage will therefore depend more strongly on the oxygen chemical potential than a structure with low coverage. The Gibbs free energy of adsorption of the clean metal surface is independent of $\Delta\mu_{\text{O}}$ and serves as a zero reference (cf. Fig. 4.5). The y-axis intercept is given by the binding energy per surface area, $-N_{\text{O}}\Delta G^{\text{bind}}_{\text{O@M}}/A$, whereas the x-axis intercept is simply given by the binding energy per oxygen atom, $\Delta G^{\text{bind}}_{\text{O@M}}$. Since the most stable structure will be the one with the lowest surface free energy, an adsorbate structure will be stable with respect to the clean surface, if $\gamma_{\text{O@M}} < \gamma_{\text{M}}$, i.e. if $\Delta G^{\text{ads}} > 0$. For plotting the Gibbs free energy of adsorption vs. the chemical potential of the gas phase the y-axis as been inverted in Fig. 4.5, so that the most stable structure always exhibits the *lowest* ΔG^{ads} . For $\Delta\mu_{\text{O}} = 0$, i.e. for very oxygen rich conditions, the adsorbate phase with the most strongly bound adsorbates will be the most stable one.

Range Of Chemical Potential

A meaningful range of $\Delta\mu_{\text{O}}$ for plotting ΔG^{ads} has to be found. As already mentioned above the stability of the different structures is compared with respect to the clean metal surface, i.e. any structure with a *higher* surface free energy (resulting in a

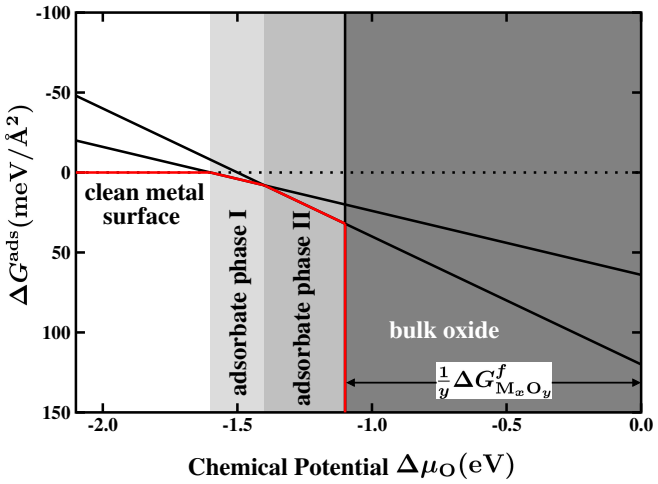

Figure 4.5: Gibbs free energy of adsorption for a surface in equilibrium with a surrounding gas phase. The clean metal surface serves as a zero reference, $\Delta G^{\mathrm{ads}} = 0$. An adsorbate phase will become stable, if its Gibbs free energy of adsorption is *lower* than the one of the clean metal surface ($\Delta G^{\mathrm{ads}} > 0$). If there is more than one adsorbate phase, always the one with the *lowest* ΔG^{ads} will be the most stable one. Here, this is indicated by the red line. With increasing gas phase chemical potential first the metal phase is stable, then the first and second adsorbate phases become stable. Finally, if $\Delta\mu_{\mathrm{O}} > \frac{1}{y}\Delta G^f_{\mathrm{M}_x\mathrm{O}_y}$, the oxide will be more stable than any adsorbate phase on the metal surface.

negative Gibbs free energy of adsorption, $\Delta G^{\mathrm{ads}} < 0$) will not be stable under the given gas phase conditions. Since all lines have a positive slope, every adsorbate phase will eventually become unstable with decreasing gas phase chemical potential. Therefore a meaningful lower bound for the gas phase chemical potential is given by the last intersection of an adsorbate phase with the clean surface, i.e. below this $\Delta\mu_{\mathrm{O}}$ the clean metal surface is always the most stable phase.

The upper bound for the oxygen chemical potential is given by the heat of formation of the corresponding bulk oxide $\Delta G^f_{\mathrm{M}_x\mathrm{O}_y}$. Since the metal oxide contains basically an *infinite* number of oxygen atoms, its stability range is marked by a vertical line. For oxygen chemical potentials greater than the heat of formation ($\Delta\mu_{\mathrm{O}} > \frac{1}{y}\Delta G^f_{\mathrm{M}_x\mathrm{O}_y}$) any oxide phase would always be thermodynamically more stable than any adsorbate phase on the metal surface.

Comparing this to the range obtained for the oxide surfaces (cf. Eq. (4.12)) it becomes obvious, that the thermodynamic stability range of the adsorbate phases ends at the point, where the stability range of the oxide surfaces begins (not considering any metastable states or kinetic effects). For the case of a metal in thermodynamic equilibrium with an oxygen gas phase one therefore usually finds the sequence *metal surface* → *adsorbate phase* → *oxide surface* with increasing oxygen chemical potential.

Evaluating The Gibbs Free Energy

The discussion of the different contributions to the Gibbs free energy is analogous to the one for the surface free energy (cf. Sec. 4.2). For the pV-term the same arguments hold, since also the Gibbs free energy of adsorption is normalized to the surface area, i.e. the pV-term will be negligible small up to rather high pressures. Also for the contribution from the configurational entropy the discussion is equivalent, since in this work the Gibbs free energy of adsorption will only be compared for several well-ordered adsorbate phases at low enough temperatures. Again for highly disordered phases the configurational entropy becomes much more important and statistical methods to sample the configurational space have to be utilized (cf. Chapter 5).

The vibrational contribution to the Gibbs free energy of adsorption can also be estimated in a similar way as for the surface free energy. As can be seen from Eq. (4.30), in contrast to the surface free energy, where the vibrational contribution was mainly determined by the difference between bulk and surface atoms, here the decisive contribution will arise from a change in the vibrational energy of molecules in the gas phase and adsorbed on the surface. This also depends on the mode of adsorption. In the case of a dissociative adsorption, as for the oxygen molecule, the O-O vibration would be *changed* into a O-M vibration, whereas for a unimolecular adsorption, as e.g. carbon monoxide, the C-O vibration would be changed and an additional C-M vibration would be introduced. In addition, if $\Delta N_{\mathrm{M}} \neq 0$, also the change in vibrational energy of metal atoms in the adsorbate structure, the clean metal surface and the bulk reservoir has to be considered.

Depending on the magnitude of the vibrational contribution and the aspired accuracy the vibrational modes of the molecules and the phonon DOS of the adsorbate phase and of the clean surface have to be evaluated to obtain the exact value. For the problems investigated in this work, an estimate of the vibrational contribution will be quantified explicitly in the second Part.

It should be stressed, that substituting the Gibbs free energy by only the total energy is in principle not necessary. In practice though evaluating all contributions to the Gibbs free energy is often too involved compared to the gain in accuracy.

4.3.2 Two-Component Gas Phases

Gibbs Free Energy Of Adsorption

The Gibbs free energy of adsorption can also be evaluated for surfaces in equilibrium with more than one gas phase component. Here this will be exemplified for a gas phase consisting of oxygen and carbon monoxide. Assuming in a first approach, that the two gas phase components do not interact with each other, the Gibbs free energy

of adsorption is given by

$$\begin{aligned}
&\Delta G^{\text{ads}}(\Delta\mu_{\text{O}}, \Delta\mu_{\text{CO}}) = \\
&= -\frac{1}{A}\left(G^{\text{surf}}_{\text{O,CO@M}} - G^{\text{surf}}_{\text{M}} - \Delta N_{\text{M}} g^{\text{bulk}}_{\text{M}} - N_{\text{O}}(1/2E^{\text{tot}}_{\text{O}_2} + \Delta\mu_{\text{O}}) - N_{\text{CO}}(E^{\text{tot}}_{\text{CO}} + \Delta\mu_{\text{CO}})\right) \\
&= -\frac{1}{A}\Delta G^{\text{bind}}_{\text{O,CO@M}} + \frac{N_{\text{O}}}{A}\Delta\mu_{\text{O}} + \frac{N_{\text{CO}}}{A}\Delta\mu_{\text{CO}} \quad .
\end{aligned} \tag{4.31}$$

Here, $\Delta G^{\text{bind}}_{\text{O,CO@M}}$ is the total binding energy of all adsorbed atoms/molecules on the surface. For a gas phase of non-interacting components the surface is then just independently in equilibrium with the two components. Since in Eq. (4.31) the Gibbs free energy of adsorption depends on two variables, one obtains a 3D-plot with a plane for each adsorbate structure instead of a line as in Fig. 4.5. The slope in x, resp. y direction only depends on the coverage of the different species. For any additional gas phase species Eq. (4.31) can simply be extended by adding the appropriate term.

To obtain the Gibbs free energy of adsorption for a surface in equilibrium with a non-interacting multi-component gas phase is thus straightforward. It is important to note that within this approach, as it is applied here, the gas phase components are assumed to be *non-interacting*, which is also called a *constrained equilibrium*, i.e. thermodynamic equilibrium is not considered between all the different subsystems. In this example thermodynamic equilibrium is only assumed between the surface and each of the two gas phases, but not between the two gas phases. If such a constraint is justified and how it influences the interpretation of the obtained results has to be discussed separately for every new system.

Bulk Oxide Stability

Considering again a metal in contact with an oxygen gas phase, the stability of the corresponding bulk oxide does usually also depend on the second gas phase component. In the case of CO as the second gas phase component, the metal oxide will eventually be decomposed into CO_2 and the metal with increasing CO content in the gas phase, which determines its stability region [82]. In a pure CO environment the stability condition of a metal oxide M_xO_y is given by

$$g^{\text{bulk}}_{\text{M}_x\text{O}_y} + y\mu_{\text{CO}} < x g^{\text{bulk}}_{\text{M}} + y\mu_{\text{CO}_2} \quad , \tag{4.32}$$

where g are the Gibbs free energies per formula unit. Approximating the chemical potential of CO_2, μ_{CO_2}, by only its total energy, $E^{\text{tot}}_{\text{CO}_2}$, Eq. (4.32) can be rearranged similar to the stability condition of a bulk oxide in the pure oxygen gas phase (cf.

Page 30), yielding

$$\begin{aligned}\Delta\mu_{\mathrm{CO}} &\lesssim -\frac{1}{y}\Delta G^{f}_{\mathrm{M}_x\mathrm{O}_y}(0,0) + E^{\mathrm{tot}}_{\mathrm{CO_2}} - E^{\mathrm{tot}}_{\mathrm{CO}} - \frac{1}{2}E^{\mathrm{tot}}_{\mathrm{O_2}} \\ &= -\frac{1}{y}\Delta G^{f}_{\mathrm{M}_x\mathrm{O}_y}(0,0) + E^{\mathrm{bind}}_{\mathrm{CO_2}} - E^{\mathrm{bind}}_{\mathrm{CO}} - \frac{1}{2}E^{\mathrm{bind}}_{\mathrm{O_2}} \\ &= -\frac{1}{y}\Delta G^{f}_{\mathrm{M}_x\mathrm{O}_y}(0,0) + \Delta E^{\mathrm{mol}} \quad ,\end{aligned} \tag{4.33}$$

with $\Delta\mu_{\mathrm{CO}} = \mu_{\mathrm{CO}} - E^{\mathrm{tot}}_{\mathrm{CO}}$. Combining this equation with the stability condition for a bulk oxide in a pure oxygen gas phase

$$\Delta\mu_{\mathrm{O}} \gtrsim \frac{1}{y}\Delta G^{f}_{\mathrm{M}_x\mathrm{O}_y}(0,0) \quad , \tag{4.34}$$

gives the stability conditions in a constrained equilibrium with a gas phase containing both oxygen and CO

$$\Delta\mu_{\mathrm{CO}} - \Delta\mu_{\mathrm{O}} < -\frac{2}{y}\Delta G^{f}_{\mathrm{M}_x\mathrm{O}_y}(0,0) + \Delta E^{\mathrm{mol}} \quad . \tag{4.35}$$

4.4 Gas Phase Chemical Potential

The surrounding gas phases are described as ideal-gas-like reservoirs. For an ideal gas the chemical potential at a given temperature T and pressure p is given by

$$\mu(T,p) = \frac{G}{N} = \frac{F+pV}{N} = \frac{-kT\ln Z + pV}{N} \quad , \tag{4.36}$$

where Z is the partition function of N indistinguishable particles

$$Z = \frac{1}{N!}\left(z^{\mathrm{trans}}\cdot z^{\mathrm{vib}}\cdot z^{\mathrm{rot}}\cdot z^{\mathrm{e}}\cdot z^{\mathrm{n}}\right)^{N} \quad . \tag{4.37}$$

z is the partition function of one gas particle. The translational, vibrational, rotational, electronic and nuclear contribution to the chemical potential can be evaluated using statistical thermodynamics [79]. Thus for any simple gas phase molecule (like O_2, CO, CO_2 etc.) the chemical potential can be directly calculated within the ideal gas approximation for any temperature and pressure. For more complicated molecules the use of tabulated values [83] might be more favorable. Since the total energy contribution to the chemical potential does not depend on temperature and pressure, it can be useful to separate $\mu(T,p)$ into the total energy and the remaining part

$$\mu(T,p) = E^{\mathrm{tot}} + \Delta\mu(T,p) \quad . \tag{4.38}$$

$\Delta\mu(T,p)$ contains then all the temperature and pressure dependent terms of μ.

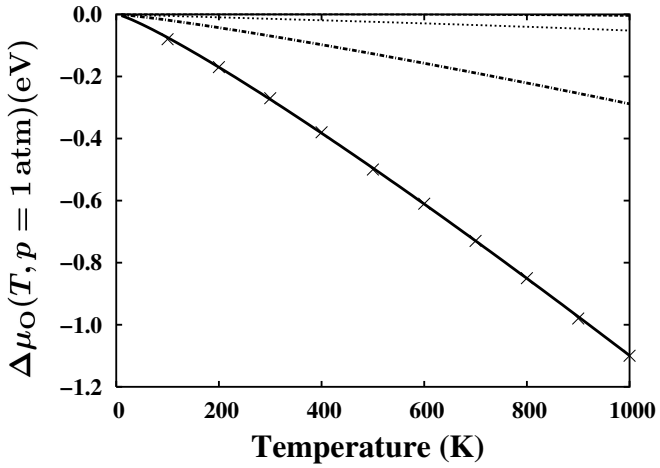

Figure 4.6: Temperature dependence of the relative oxygen chemical potential $\Delta\mu_O(T, p)$ at $p = 1\,\mathrm{atm}$. Compared are the tabulated values from Ref. [83] (crosses) to the calculated ones within the ideal gas approximation. Additionally shown are the sums of the individual contributions: vibrational (dashed line, almost coinciding with the zero axis), vibrational+nuclear (dotted line), vibrational+nuclear+rotational (dash-dotted line). The remaining large difference to the full result (solid line) is due to the translational contribution (from Ref. [84])

The approximation of the real gas phase by an ideal gas will only introduce a negligible error in the temperature and pressure range considered in this work, which can be shown by comparing the calculated values within the ideal gas approximation to the experimentally derived, tabulated ones [83]. In Fig. 4.6 this is illustrated for the for the (T, p)-dependent part of the oxygen chemical potential $\Delta\mu_O(T, p)$ at a pressure of $p_{O_2} = 1\,\mathrm{atm}$ and temperatures up to $T = 1000\,\mathrm{K}$.

4.5 Summary

Combining DFT calculations with thermodynamic concepts provides a very useful tool to extend the knowledge gained in the microscopic regime to the meso- and macroscopic properties of a system. This approach can be used to describe systems that are in thermodynamic equilibrium, but it does not contain information about the kinetics involved to reach the final equilibrated state. Also open systems in a *steady state*, which is governed by a continuous supply and removal of particles, can not be described within this approach. Nevertheless identifying the thermodynamic equilibrium state can often already provide a first, valuable insight into a given system.

The general concept of *ab initio atomistic thermodynamics* is illustrated using the surface free energy and the Gibbs free energy of adsorption as example. In addition the different contributions to the Gibbs free energy have been discussed. Here, it

is important to note, that the magnitude of the different contributions has to be carefully evaluated for every system. Usually a coarse estimate of an upper bound of the contributions besides the total energy can be obtained rather easy, whereas the exact calculation of all contributions to the Gibbs free energy can become fairly involved.

The atomistic thermodynamics approach, as it is outlined here, is an indirect approach, i.e. it can only be used to *compare* different structures, but it will not predict any new phases. Thus, having a given set of experimentally and/or theoretically proposed structures their thermodynamic stability can directly be compared over a wide range of temperature and pressure conditions. Also any new suggested structure can then be included at a rather low computational cost. But all obtained results are only valid within the restricted set of investigated structures, i.e. any configuration that is not considered within this set of structures can also not appear as a stable structure. Therefore, it is important to compare a rather large set possible configurations, at least including all experimentally identified ones, but still it can not be excluded, that an important structure might have been missed. Nevertheless the advantage of this approach is the relatively small computational demand, so that a first insight from the thermodynamic description can be obtained rather fast.

In the following Chapter an approach considering statistical mechanics is discussed, which can overcome some of the drawbacks of the atomistic thermodynamics approach, but is usually much more costly.